AIP | Journal of Applied Physics

Growth and luminescence properties of micro- and nanotubes in sintered tin oxide

D. Maestre, A. Cremades, and J. Piqueras

Citation: J. Appl. Phys. **97**, 044316 (2005); doi: 10.1063/1.1851602
View online: http://dx.doi.org/10.1063/1.1851602
View Table of Contents: http://jap.aip.org/resource/1/JAPIAU/v97/i4
Published by the American Institute of Physics.

Growth and luminescence properties of micro- and nanotubes in sintered tin oxide

D. Maestre, A. Cremades, and J. Piqueras[a)]
Departamento de Física de Materiales, Facultad de Ciencias Físicas, Universidad Complutense de Madrid, 28040 Madrid, Spain

(Received 7 September 2004; accepted 30 November 2004; published online 28 January 2005)

Sintering SnO_2 under argon flow at temperatures in the range of 1350–1500 °C causes the formation of wires, rods, and tubes on the sample surface. At high temperatures of the mentioned range, microwires with lengths of hundreds of microns are formed. At lower temperatures the formation of micro- and nanorods as well as micro- and nanotubes takes place. The influence of ball milling of the starting powder on the formation of tubes is investigated. The local cathodoluminescence measurements show a different defect structure in the tubes than in the sample background. © *2005 American Institute of Physics*. [DOI: 10.1063/1.1851602]

I. INTRODUCTION

Fabrication and characterization of semiconductor structures in form of nanowires, nanorods, or nanotubes are subjects of increasing interest due to the potential applications of such nanostructures in future nanoelectronics systems. In the particular case of semiconductor oxides, other applications as in transparent electrodes or in gas sensing devices are also of interest. ZnO has attracted much attention, and the growth of different one-dimensional nanostructures of this semiconductor has been reported in the past years.[1–5] Low dimensional nanostructures of other semiconductor oxides with gas sensing applications, such as Ga_2O_3, TiO_2, and SnO_2, have been also developed. The high surface-to-volume ratio of the nanostructures provides a high sensitivity to the interaction with gases. For instance, nanowires, nanoribbons, and nanotubes of Ga_2O_3 and TiO_2 have been synthesized by different methods.[6–9] However, there are only few reports on the fabrication of similar structures of SnO_2, which is known to be an important material for gas sensors and optoelectronic devices. Dai *et al.*[10] have synthesized long single-crystalline SnO_2 nanoribbons by thermal evaporation of SnO and SnO_2 powders at high temperature. In Ref. 11 the formation of tin oxide nanowires, nanoribbons, and nanotubes and the electron microscopy characterization of these structures are reported. The synthesized nanotubes had diameters between 50 and 350 nm with a noncontinuous hollow core.

In this work the growth of tubes on the surface of sintered SnO_2 during sintering treatments is investigated. The cross-sectional dimensions of the tubes range typically from several microns to hundreds of nanometers. SnO_2 tubes are found to exhibit unique optical properties, as measured by cathodoluminescence in the scanning electron microscopy (SEM).

The morphology and size of the tubes as a function of the temperature of treatment have been investigated by SEM, while additional characterization was performed by cathodoluminescence (CL) in the SEM and by x-ray diffraction (XRD).

[a)]Electronic mail: piqueras@fis.ucm.es

II. EXPERIMENTAL METHOD

The starting material used was commercial SnO_2 powder (Aldrich Chemical Company Inc., 99.9% purity). The powder consists of particles and aggregates of rounded particles with sizes of about 200 nm. The samples were prepared by compacting the powders under a compressive load of 2 tons to form disks of about 7-mm diameter and 2-mm thickness. The samples were then sintered in a static air or under air or argon flow at temperatures between 1000 and 1500 °C. Some samples were sintered with powder which had been milled in a centrifugal ball mill, Retsch S100, with 20-mm-diameter agate balls for 100 h. This treatment leads to a smaller and more homogeneous particle size. The size after 30-h milling was about 130 nm and slightly smaller after 60- and 100-h milling.

The samples were observed in the secondary electron and CL modes in a Hitachi S-2500 or a Leica 440 SEM at beam voltages ranging from 10 to 30 keV at a temperature of 80 K. For the CL measurements (images and local spectra) recorded on tubes and other elongated structures a low beam voltage has been used in order to obtain luminescence only from the chosen structures or faces. For the CL images a Hamamatsu R-928 photomultiplier was used. The CL spectra were recorded either with the photomultiplier tube attached to an Oriel 78215 monochromator or with a charge-coupled device camera with a built-in spectrograph (Hamamatsu PMA-11). Additional structural information on the samples was obtained by x-ray diffraction (XRD).

III. RESULTS AND DISCUSSION

The particle size of samples sintered in static air ranged from about 200 nm after the 1000 °C treatment to about 100 μm in samples sintered at 1500 °C. In samples prepared from a ball milled powder, the particle size varied from about 130 nm to about 60–70 μm in the same temperature range of sintering. We have previously reported[12] that the CL spectra and CL intensity of the samples depend on the annealing temperature. In the different spectra, luminescence bands centered at about 1.94, 2.25, and 2.58 eV were observed. In

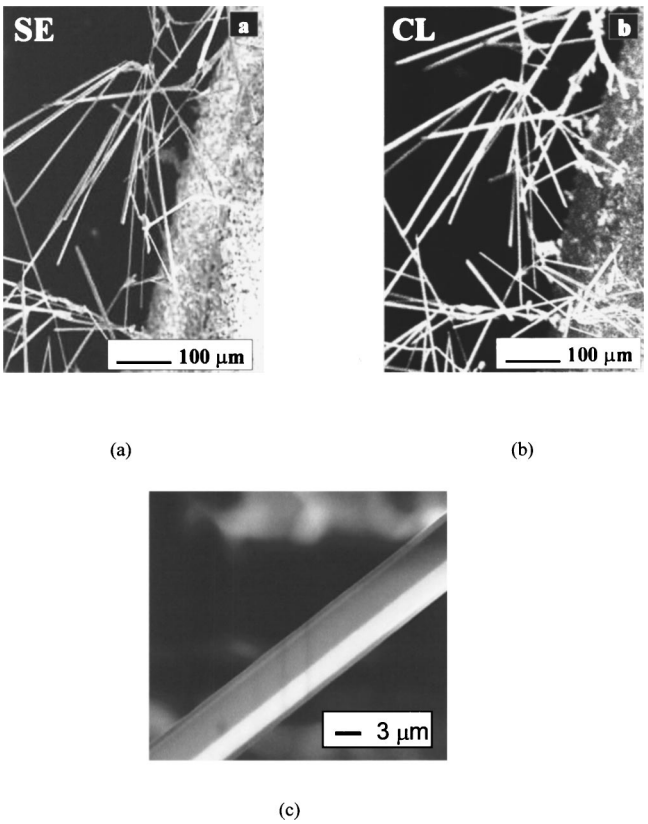

FIG. 1. SEM (a) and CL (b) images of wires on a sample sintered at 1500 °C in argon flow. (c) Detail of a wire appearing on a sample sintered at 1500 °C in argon flow.

the CL spectra of the starting powder and of samples sintered at temperatures up to 1200 °C the 1.94 eV is the main band, while after sintering at higher temperatures either the emission at 2.58 eV or at 2.25 eV become dominant. Mechanical milling also induces strong changes in the relative intensity of the CL bands at 1.94 and 2.58 eV. Further details on the dependence of the CL spectra on annealing temperature and milling treatment were also reported in Ref. 12. In this work we report the new tubular structures growing in the samples during annealing under a moderate flow of argon.

Sintering untreated powder at 1500 °C for 10 h under argon flow leads to the formation of a wirelike structure on the sample surface. Typical cross-sectional dimension of the wires is several microns and the length is of hundreds of microns or even reach the millimeter range. Figure 1(a) shows a SEM image of the wire distribution on the surface. The CL image of Fig. 1(b) shows an enhanced emission from the wires, as compared with the sample surface. In the SEM [Fig. 1(c)] a detail of a wire presenting facetted surface is observed. The presence of the wire morphology does not influence the overall CL spectra, which are similar for the samples sintered in static air and in argon flow. Both spectra have a dominant emission at 2.25 eV with a higher intensity in the samples treated in argon. The CL images of the surface show similar appearance in both samples, treated in air or in argon, with enhanced emission at the grain boundaries.

In order to study the early stages of wire formation, sintering treatments in argon at lower temperatures were carried out in 50 °C steps. It has been found that the first structures,

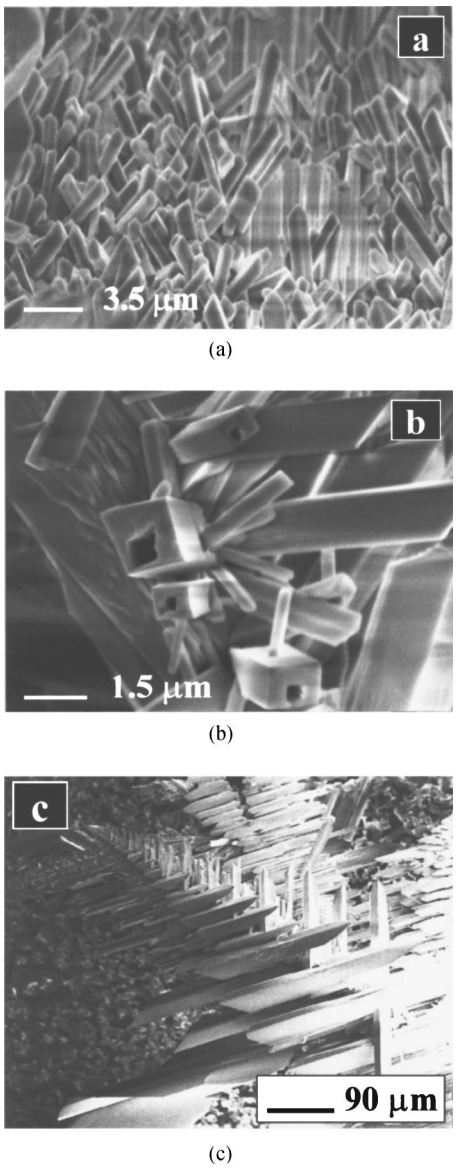

FIG. 2. (a) Microrods and (b) tubes grown after a treatment at 1350 °C in argon flow. (c) Microstructures appearing on samples sintered at 1400 °C in argon flow with a preferent growth direction.

with different shapes and dimensions, which can be related to the growth of wires appear after the 1350 °C treatment, preferently at the edge of the disk. Some areas of the sample appear covered by micro- and nanorods with a rectangular section [Fig. 2(a)]. Some of the rods have a tubular structure with thick walls and hollows with different shapes, as Fig. 2(b) shows. In other regions of the sample, the structures appear with a flowerlike or branch appearance including rods and tubes with a broad range of dimensions as well as needlelike crystals. XRD of all the samples revealed that no new phases appear during the treatments.

In the samples treated at 1400 or 1450 °C, rods and tubes are distributed over the whole sample surface and not only at the disk edges. The main structures formed during these treatments are rods and tubes of different sizes, with rectangular cross section and well-defined lateral faces. Based on an analysis of the surface energy in several crystallographic orientations Beltran *et al.*[13] obtained the stability

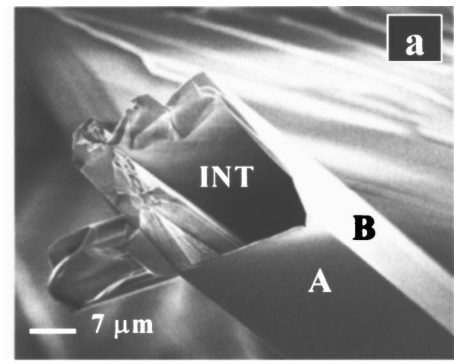

(a)

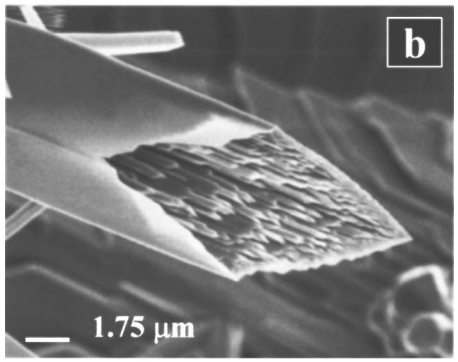

(b)

FIG. 3. SEM images of tubes in samples sintered at 1400 °C in argon flow, showing inner scale structure (a) and perfectly oriented layered nanostructures (b).

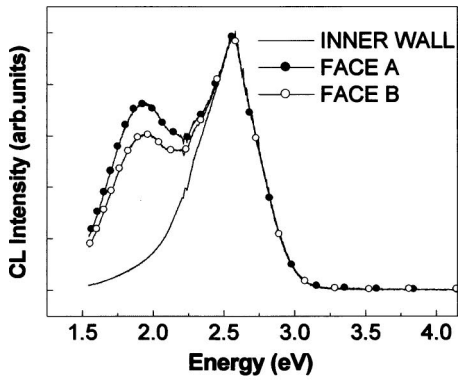

(a)

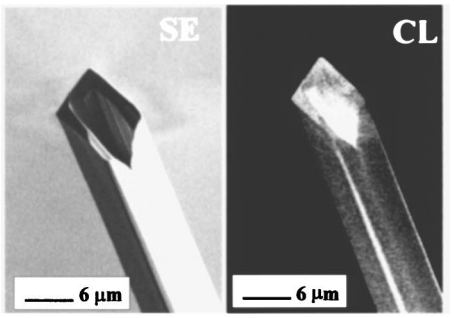

(b)

FIG. 4. (a) CL spectra recorded in different crystal faces and in the inner wall of the tube shown in the Fig. 3(a). (b) SEM and CL images of a tube on a sample sintered at 1400 °C in argon flow.

conditions of the different stoichiometric surfaces and the energetic cost associated with the combination of these surface to form nanoribbons. Their calculations indicate that the (110) surface is the most stable which is in agreement with the fact that it is one of the dominant surfaces of our polycrystalline sample, as measured by XRD. The (001) and (201) planes have a relative higher surface energy, which may lead to a growth along the directions of [001] and [201], respectively. On the other hand, the (100), (010), (101), and (10-1) surfaces are more stable to be the preferred orientation of the nanoribbon side surfaces. Taking into account that our tubes show a rectangular cross section and according to the discussion of Ref. 13, the most probable growth direction seems to be the [101]. The narrow and the wide lateral surfaces of the rectangular tube would be the (010) and (10-1) planes, respectively, as the (10-1) plane has a lower free formation energy and can be developed more readily. Similar results have been obtained for nanoribbons by Dai *et al.*[10,11] and Law *et al.*[14] In some areas no preferent growth direction is observed, in the micro- and nanostructures, while in other regions the structures are oriented along preferent directions [Fig. 2(c)]. The external faces of the tubes are normally flat, as observed in the SEM, while the interior of the tubes can present different appearances which possibly correspond to different stages of the growth process. This is readily observed for the larger tubes, as those shown in Fig. 3. In Fig. 3(a) the inner wall shows a scale or layered structure while the tube shown in Fig. 3(b) is filled with a perfectly oriented layered nanostructure.

The presence of the tubes with large dimensions enables us to record spectra in different crystal faces as well as in the tube interior. Figure 4(a) shows the spectra recorded in the faces and in the inside walls of the tube shown in Fig. 3(a). It can be appreciated that the spectrum of the internal face consists of a single band centered at 2.58 eV while in the external faces bands at 1.94 and 2.25 eV are also observed. CL images of Fig. 4(b) reveal that the inner part of the tubes emits with higher intensity (2.58 eV) than the external faces (1.94, 2.25, and 2.58 eV) and that of the sample background. The luminescence emission from the internal regions of nanotubes is of potential application in high-resolution displays as, for instance, in the case of carbon nanotubes containing ruthenium–iron particles.[15] The higher luminescence of the internal surfaces is not due to the different crystallographic orientations but to the defect structure resulting from the growth process, as observed in the different spectra recorded on the internal and external side of the same tube faces shown in Fig. 4. The complex inner ordered nanostructures related to the first stages of the tube growth, shown in Fig. 3, could be related to this unique luminescence property of the tubes. The 2.58-eV band has been previously reported for SnO_2,[16,17] but it was not normally considered to be inde-

pendent of the green (2.25 eV) or orange (1.94 eV) emissions. We have previously[12] associated the 2.58-eV band to certain crystal faces in samples sintered at 1500 °C, and we found that this band is not a component of the 1.94-eV band which has been associated to oxygen vacancies.

Comparison of the samples prepared from untreated powder and from milled powder shows that in both cases the above-described structures are formed. However, when milled powder is used as starting material the samples are more homogeneous and most of the structures formed are the rectangular rods or tubes while other more complexes structures, as the above-mentioned flowerlike are only occasionally observed. It appears that reducing the crystallite size during the milling process, increases the number of nucleation centers and crystallites, with orientation favorable for the growth of the observed elongated structures. This fact is of significant importance in order to fabricate at a large scale homogeneously distributed and ordered tube structures with dimensions up to hundreds of microns length and cross sections from tens of microns down to a nanometer scale. The influence of other sintering parameters on the formation of tubes, wires, and rods has been preliminarily studied. It has been found that a reduction of the sintering time leads to a strong reduction of the number of the structures. In samples treated in argon at 1500 °C for 2.5 h, only few elongated structures are present while after 10-h treatment the surface [shown in Fig. 2(a)] is covered with wires. It has been already mentioned that the same thermal treatments performed under static air do not lead to the structures described here, which are formed only when a flow is present. Similar experiments performed under an air flow also lead to the formation of the structures. However, under our experimental conditions the tubes and rods were more homogeneously distributed and with better defined shapes when the samples were treated in argon.

The thermal evaporation of powders under a gas flow followed by a deposition on a substrate has been reported as a method to obtain nanostructures as nanowires, nanorods, or nanotubes of different oxides e.g.,.[1,3,10,11] Pan *et al.*[1] concluded that the growth of their nanobelts does not take place by the vapor–liquid–solid process which was proposed[18] for the growth of nanowires by a catalyst-assisted technique.[19] Instead, they proposed that the growth was governed by a vapor–solid process,[20] in which the oxide vapor evaporated from the starting oxide directly deposits on a substrate at a lower-temperature region. In our case the source is a compacted disk of oxide which is also the substrate for the micro- and nanostructures. Since not a catalytic process or a foreign substrate is involved it is suggested that the formation of the structures takes place by a vapor–solid process.

IV. CONCLUSIONS

Sintering of SnO_2 compacted disks under argon flow in the temperature range of 1350–1500 °C leads to the formation of SnO_2 wires, rods, and tubes on the sample surface. The particular morphology of the one-dimensional structures depends on the specific treatment. Wires are formed at 1500 °C, while micro- and nanotubes with rectangular cross section are formed at lower temperatures and appear in some areas with preferential growth directions. Ball milling of the starting powder has been found to favor the homogeneity of the final structure. The local cathodoluminescence measurements reveal a different spectral output from the tubes than from the surface background as well as a dependence of emission on the tube face considered. In particular, enhanced luminescence emission arises in the internal surface of the tubes.

ACKNOWLEDGMENT

This work is supported by MCYT (Project No. MAT 2003-00455)

[1] Z. W. Pan, Z. R. Dai, and Z. L. Wang, Science **291**, 1947 (2001).
[2] H. T. Ng, B. Chen, J. Li, J. Han, M. Meyyappan, J. Wu, S. X. Li, and E. E. Haller, Appl. Phys. Lett. **82**, 2023 (2003).
[3] J.-S. Lee, K. Park, M.-Il Kang, I.-W. Park, S.-W. Kim, W. K. Cho, H. S. Han, and S. Kim, J. Cryst. Growth **254**, 423 (2003).
[4] J. Q. Hu and Y. Bando, Appl. Phys. Lett. **82**, 1401 (2003).
[5] Y. J. Xing *et al.*, Appl. Phys. Lett. **83**, 1689 (2003).
[6] H. Z. Zhang *et al.*, Solid State Commun. **109**, 677 (1999).
[7] Y. C. Choi *et al.*, Adv. Mater. (Weinheim, Ger.) **12**, 746 (2000).
[8] S. Sharma and M. K. Sunkara, J. Am. Chem. Soc. **124**, 12288 (2002).
[9] G. H. Du, Q. Chen, R. C. Che, Z. Y. Yuan, and L. M. Peng, Appl. Phys. Lett. **79**, 3702 (2001).
[10] Z. R. Dai, Z. W. Pan, and Z. L. Wang, Solid State Commun. **118**, 351 (2001).
[11] Z. R. Dai, J. L. Gole, J. d. Stout, and Z. L. Wang, J. Phys. Chem. B **106**, 1274 (2002).
[12] D. Maestre, A. Cremades, and J. Piqueras, J. Appl. Phys. **95**, 3027 (2004).
[13] A. Beltrán, J. Andrés, E. Longo, and E. R. Leite, Appl. Phys. Lett. **83**, 635 (2003).
[14] M. Law, H. Kind, B. Messer, F. Kim, and Y. Yang, Angew. Chem. **114**, 2511 (2002).
[15] E. C. Dickey, C. A. Grimes, M. K. Jain, K. G. Ong, D. Qian, P. D. Kichanbare, R. Andrews, and D. Jacques, Appl. Phys. Lett. **79**, 4022 (2001).
[16] J. P. Fillard and M. de Murcia, Phys. Status Solidi A **30**, 279 (1975).
[17] S. S. Chang and D. K. Park, Mater. Sci. Eng., B **95**, 55 (2002).
[18] R. S. Wagner and W. C. Ellis, Appl. Phys. Lett. **4**, 89 (1964).
[19] A. M. Morales and C. M. Lieber, Science **279**, 208 (1998).
[20] P. Yang, C. M. Lieber, J. Mater. Res. **12**, 2981 (1997).